PROCEEDINGS OF SPIE

SPIEDigitalLibrary.org/conference-proceedings-of-spie

Towards development of fibre-optic surface enhanced Raman spectroscopy probes using 2-photon polymerisation for rapid detection of bacteria

Jang Ah Kim, Dominic J. Wales, Alexander J. Thompson, Guang-Zhong Yang

Jang Ah Kim, Dominic J. Wales, Alexander J. Thompson, Guang-Zhong Yang, "Towards development of fibre-optic surface enhanced Raman spectroscopy probes using 2-photon polymerisation for rapid detection of bacteria," Proc. SPIE 10894, Plasmonics in Biology and Medicine XVI, 108940F (7 March 2019); doi: 10.1117/12.2507961

SPIE.

Event: SPIE BiOS, 2019, San Francisco, California, United States

Downloaded From: https://www.spiedigitallibrary.org/conference-proceedings-of-spie on 11 Mar 2019 Terms of Use: https://www.spiedigitallibrary.org/terms-of-use

Towards development of fiber-optic surface enhanced Raman spectroscopy probes using 2-photon polymerization for rapid detection of bacteria

Jang Ah Kim*[a], Dominic J. Wales[a], Alex J. Thompson[b], Guang-Zhong Yang[a]
[a]The Hamlyn Centre, Imperial College London, Exhibition Road, South Kensington, London, SW7 2AZ, UK; [b]The Hamlyn Centre, Surgical Innovation Centre (Paterson Building), Dept. of Surgery & Cancer, St. Mary's Hospital, Imperial College London, South Wharf Road, London, W2 1NY, UK

ABSTRACT

In this study, a variety of direct laser written surface-enhanced Raman spectroscopy (SERS) micro-structures, designed for bacteria detection, are presented. Various SERS micro-structures were designed to achieve both a high density of plasmonic hot spots and a strong probability of interaction between the hot spots and the target bacterial cells. Two-photon polymerization was used for initial fabrication of the polymeric skeletons of the SERS micro-structures, which were then coated with a 50 nm-thick gold layer via e-beam evaporation. The micro-structures were fabricated on glass coverslips and were assessed using a confocal Raman microscope. To this end, Rhodamine 6G was used as an analyte under 785 nm laser illumination. The optimal SERS micro-structures showed approximately 2×10^3 enhancement in Raman signal (analytical enhancement factor, AEF) at a wavenumber of 600 cm^{-1}. Real-time detection of *E. coli* in solution was demonstrated using the fabricated SERS platform with low laser powers and a short acquisition time (785 nm, 5 mW, 50 ms).

Keywords: surface-enhanced Raman spectroscopy, plasmonic hot spots, two-photon polymerization, direct laser writing, bacteria detection

1. INTRODUCTION

In the last couple of decades, Raman (scattering) spectroscopy has been proven to be a powerful tool for non-destructive molecular analysis in many fields – for instance, mineralogy[1], material science[2,3], semiconductor industry[4], pharmacy[5], and forensic science[6,7] – because it provides a high accuracy and does not require exogenous labelling. The life sciences have benefitted from the use of Raman spectroscopy for analysis due to its insensitivity to water molecules, which are abundant and thus cause huge interference in the analysis of biological analytes[8]. Hence, substantial studies on Raman spectroscopy of various biological samples, such as biofluids[9] and tissues[10], either *in vitro* or *in vivo*, have been actively carried out, demonstrating the capability for a range of diseases. However, there has always been a necessity to improve the signal collection efficiency to overcome the fundamentally weak signal strength of Raman scattering compared to other scattering processes (e.g. Rayleigh scattering)[11]. To this end, various techniques, such as surface-enhanced Raman spectroscopy (SERS), tip-enhanced Raman spectroscopy (TERS), stimulated Raman spectroscopy (SRS), resonance Raman spectroscopy (RRS), which enhance the intrinsic Raman scattering signal, have been developed. Among these techniques, SERS is the one that has been investigated most actively and reported widely. The SERS effect is produced from either roughened metal surfaces or metal nanoparticles (NPs). Conventionally, noble metals (e.g. Au, Ag, etc.) are used because they are rich in free electrons that can generate surface plasmons by resonating with incident light under certain excitation conditions. These surface plasmons give rise to tightly confined localized electromagnetic (EM) fields (called "hot spots") that act as oscillating dipoles serving to amplify the intrinsic Raman signal when an analyte molecule is close enough to the metal surface[12]. Typically, hot spots can be formed at nanogaps, nanotips, and edges, therefore colloidal NPs and NP-deposited or nano-patterned planar substrates have been used for SERS measurements. Fabrication of these SERS platforms often involves multiple steps, chemical processes and/or nano-fabrication techniques (e.g. electron-beam lithography, focused-ion beam, photolithography, etc.). Importantly, the controllability, homogeneity and reproducibility of the fabricated platforms, as well as the versatility and efficiency of the processes, are crucial aspects

*j.a.kim@imperial.ac.uk; https://www.imperial.ac.uk/hamlyn-centre/

Plasmonics in Biology and Medicine XVI, edited by Tuan Vo-Dinh, Ho-Pui A. Ho, Krishanu Ray, Proc. of SPIE
Vol. 10894, 108940F · © 2019 SPIE · CCC code: 1605-7422/19/$18 · doi: 10.1117/12.2507961

Downloaded From: https://www.spiedigitallibrary.org/conference-proceedings-of-spie on 11 Mar 2019
Terms of Use: https://www.spiedigitallibrary.org/terms-of-use

when employing those SERS platforms for practical applications[13].

In this study, a set of SERS micro-structures fabricated using direct laser writing (DLW) – a micro-scale 3D printing technique based on two-photon polymerization (2PP) – is presented. DLW has been used extensively in several fields due to its versatility in terms of achievable length scales and morphologies, encompassing micro- to meso-scales and both 2D and 3D structures. In particular, this technique has been actively used within optics and photonics due to the ability to fabricate 3D, micro-scale, optically transparent structures. For this reason, DLW was used here to generate the polymer skeletons of various 2D and 3D micro-structures designed to produce numerous effective SERS hot spots (once coated with a noble metal). Electron-beam deposition was then performed to deposit a thin film of Au onto the printed polymer skeletons. Subsequently, the SERS characteristics of the fabricated micro-structures were evaluated using Rhodamine 6G. Finally, preliminary assessment of the capability for rapid detection of *E. coli* was performed using the SERS micro-structure exhibiting the highest signal enhancement. The aim of the presented experiments was to demonstrate and characterize a simple, repeatable, two-step fabrication protocol for SERS micro-structures that could later be translated to the development of SERS structures on optical fiber tips.

2. EXPERIMENTAL DETAILS

2.1 SERS micro-structures fabrication process

A Photonic Professional GT2 (Nanoscribe GmbH, Germany) 2PP system was employed to create polymer skeletons of various SERS micro-structures. Microscope glass coverslips (22 mm × 22 mm) were initially cleaned with acetone, isopropyl alcohol (IPA) and then distilled water before being gently dried under a stream of nitrogen gas. Cleaned coverslips were then placed in a solution of 3-(trimethoxysilyl)propyl methacrylate (Sigma-Aldrich) (0.5 mL) in ethanol (25 mL) and left for at least 2 hours for an additional surface treatment to enhance the adhesion of a photoresist on the glass coverslips. Once complete, the coverslips were rinsed and dried again, as described above and then fixed on the substrate holder with polyimide adhesive tape. Subsequently, a drop of the index matching immersion oil and a drop of the photoresist (IP-L 780, Nanoscribe GmbH) were applied on the bottom and the top of the coverslips, respectively. The substrate holder was then placed on the microscope (63× objective) and the focus at the interface between the surface of the coverslip and the photoresist was optimized by finding the optical interference caused by the difference in the refractive index. Prior to printing, the geometries of the micro-structures were generated either by manually programming job scripts using DeScribe, a software package provided along with the Nanoscribe 2PP system, or by importing STL files of 3D models created in SolidWorks (Dassault Systèmes, France). In this study, models with a 2D single-voxel array were fabricated using the former method, whereas printing of other more complicated models employed the latter approach. Once a printing job was complete, the coverslips were soaked in propylene glycol methyl ether acetate (PGMEA) for 20 min for development and then immersed in isopropyl alcohol for another 2 min to complete the removal of the uncured photoresist residue. SERS-active micro-structures were then created by depositing a 50 nm-thick gold thin film (electron beam deposition) on the printed polymer skeletons using a thin film deposition system (HEX, Korvus Technology, UK). The microscopic details of the SERS micro-structures were observed under a field enhanced-scanning electron microscope (FE-SEM, LYRA3, Tescan, s.r.o., Czech Republic).

2.2 Raman spectroscopy

Characterization of the fabricated SERS micro-structures was performed using a Raman imaging microscope (DXR^{TM}2xi, Thermo Fisher Scientific Inc.). Rhodamine 6G (R6G, Sigma-Aldrich) aqueous solution was used to assess the enhancement characteristics of the structures. A droplet of R6G aqueous solution (0.5 mM) was placed on the area where the SERS micro-structures were printed and covered with another cleaned coverslip fixed with a microscope spacer seal to avoid rapid evaporation of the solution. Then, the sample coverslip was transferred to the microscope. A long working-distance 50× objective lens was used to scan the area that contained the SERS micro-structure arrays. Raman spectra were recorded by illuminating the micro-structures with a 785 nm laser, using a laser power of 10 mW at the sample and an exposure time of 10 ms. 2D imaging of Raman spectra was carried out with a 1.0 um pixel size and averaged for 3 scans.

Meanwhile, a reference Raman spectrum of R6G without SERS was required to calculate the enhancement factors (EFs) of each micro-structure. A higher concentration R6G aqueous solution was used to take the reference spectrum. A droplet of 10 mM R6G solution was placed on a glass slide wrapped with Al foil and secured with a coverslip and a microscope spacer seal as described above. Additionally, a longer exposure time of 667 ms was employed for the non-SERS measurements to allow spectra to be collected with acceptable signal-to-noise ratios.

Downloaded From: https://www.spiedigitallibrary.org/conference-proceedings-of-spie on 11 Mar 2019
Terms of Use: https://www.spiedigitallibrary.org/terms-of-use

2.3 Spectroscopic data processing

The spectra from every SERS micro-structure were averaged over the scanned areas (approx. 50 μm × 50 μm, > 2,500 spectra) while the R6G reference spectrum was taken by averaging over the spectra taken from 10 random positions. For subtracting the broad background from the spectra, an asymmetric least square (ALS) smoothing technique was used. Once the background was subtracted, the wavenumbers and intensities of prominent peaks were elicited to calculate the analytical EFs (AEFs) as

$$\text{AEF}=\frac{I_{SERS}/C_{SERS}}{I_{RS}/C_{RS}} \tag{1}$$

where I_{SERS} and C_{SERS} respectively represent the peak intensity and analyte concentration for the SERS measurements, and I_{RS} and C_{RS} represent the equivalent values for the Raman scattering (non-SERS) measurements. It is important to note here that the AEF cannot completely characterize SERS substrates because surface effects (e.g. molecular coverage and surface adsorption, which provide some of the main contributions to the SERS signal) are ignored. Thus, it is strongly dependent on not only the molecular species but also the sample preparation procedure. Despite this, the AEF offers a simple figure for the signal enhancement that can be expected when in any practical analytical situation[14–16]. Finally, a further normalization was performed to correct for the use of different laser powers (*LP*) and acquisition times (*t*) for SERS and non-SERS conditions as shown below.

$$\text{Normalized AEF}=\frac{\left(\frac{I_{SERS}}{LP_{SERS}\times t_{SERS}}\right)/C_{SERS}}{\left(\frac{I_{RS}}{LP_{RS}\times t_{RS}}\right)/C_{RS}} \tag{2}$$

The normalized AEFs for each main peak of the R6G spectra from the different SERS micro-structures were then compared and analyzed.

2.4 *E. coli* bacteria detection

To provide a preliminary assessment of the capability of the fabricated SERS micro-structures for rapid bacteria detection, wild type laboratory strain *Escherichia coli* (*E. coli* K-12, MG-1655) were cultured (in lysogeny broth, 37°C, overnight, shaking) until saturated (~10^9 cells/mL) and applied on the sample coverslips as described in section 2.2. Since live *E. coli* were used in these experiments, a lower laser power of 5 mW was used to avoid damage to cells. Furthermore, as the cells were motile, shorter signal acquisition times (5 ms exposure time, average of 10 scans) and point-based rapid spectrum monitoring were used to capture spectra of the swimming bacteria.

3. RESULTS AND DISCUSSIONS

3.1 Design and fabrication parameters

The unit geometries and SEM micrographs of the three different micro-structure arrays that were examined in this study are presented in Fig. 1. To generate gaps and tips that can form SERS hot spots using DLW, three structures were proposed: basic arrays of single voxels, arrays of hierarchical pyramids, and arrays of tree-like structures. The basic single-voxel array (BSVA, Fig. 1 (a)-(c)) was designed to replicate conventional 2D self-assembled metallic NP SERS arrays, which are common in the literature. For the BSVA, single-voxels were generated at the surface of the glass coverslip by exposing a point coordinate with the laser. Two different spacings between voxels (a = 0.6 μm and a = 0.9 μm) were compared in order to demonstrate the effect of varying the size of the gaps between voxels.

As an aside, it is noteworthy here that the NPs used in NP SERS arrays are generally smaller than the smallest features achievable using the Nanoscribe 2PP system. However, as 2PP does not require any chemical fabrication, it offers potential advantages over conventional fabrication techniques in terms of both ease and repeatability of manufacturing.

To investigate the SERS effects obtained with more complex structures, 3D models of hierarchical pyramid arrays (HPA, Fig. 1 (d)-(f)) and arrays of tree-like structures (TA, Fig. 1 (g)-(i)) were designed using SolidWorks. As shown in Fig. 1, when overlapped in arrays these structures provided multiple sizes/spacings of tips and gaps, with the aim of offering improved signal enhancement (relative to the BSVA). To demonstrate the effect of the scale of the HPAs, a second HPA was fabricated at half the size (HPA_1/2x). Furthermore, two different TA patterns (TA1 and TA2) were also fabricated (see Fig. 1 (h&i)). As described above, all micro-structures were tested to determine their SERS characteristics.

Downloaded From: https://www.spiedigitallibrary.org/conference-proceedings-of-spie on 11 Mar 2019
Terms of Use: https://www.spiedigitallibrary.org/terms-of-use

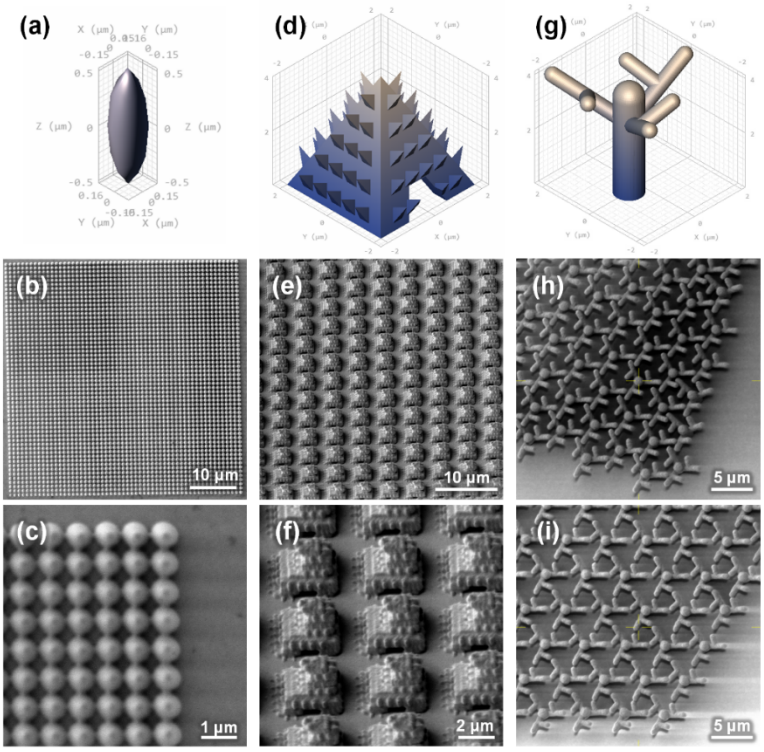

Figure 1. 3D models and SEM micrographs of the SERS micro-structure arrays proposed and examined in this study: 2D basic single-voxel array (BSVA) (a-c), hierarchical pyramid array (HPA) (d-f), and tree array (TA) (g-i). (a) The theoretically predicted geometry of a voxel. (b) SEM micrograph of 2D BSVA with a spacing distance a = 0.9 µm and (c) detail view. (d) 3D modelling of a hierarchical pyramid, (e) tilted SEM micrograph of a HPA and (f) detail view of a HPA with a spacing distance a = 4.611 µm. (g) 3D modelling of a tree-like structure. (h-i) Two different TAs: (h) TA1, (i) TA2.

3.2 Comparison of SERS micro-structures and AEFs

R6G spectra were recorded using all micro-structures. Fig. 2 shows characteristic spectra recorded using the BSVA. There was a residual common interference background, even after baseline correction (Fig. 2 (b)), which was attributed to the band-pass filter behaving as an etalon. Representative vibration modes of the R6G molecule were found at wavenumbers of 600 cm^{-1} (C – C – C ring in-plane vibration), 762 cm^{-1} (C – H out-of-plane bending), 1172 cm^{-1} (C – H in-plane bending), 1300 cm^{-1} (N – H in-plane bending), 1350 cm^{-1} and 1500 cm^{-1} (C – C stretching).

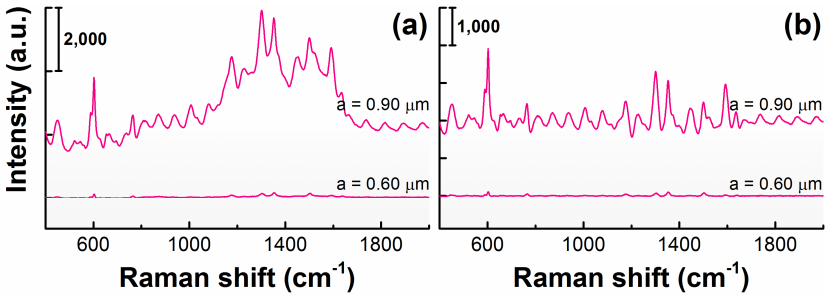

Figure 2. Raman spectra of 0.5 mM R6G aqueous solution on the 2D BSVAs with different spacing distances, 0.6 µm and 0.9 µm. (a) Area-averaged raw data over each array before post-processing of the spectra. (b) Baseline corrected spectra with asymmetric least squares smoothing.

Downloaded From: https://www.spiedigitallibrary.org/conference-proceedings-of-spie on 11 Mar 2019
Terms of Use: https://www.spiedigitallibrary.org/terms-of-use

To evaluate the SERS performance of the micro-structures, Fig. 3 shows a characteristic R6G spectrum recorded using each structure along with a reference spectrum recorded on foil. In addition, the peak intensities from the best spectrum from each structure were extracted and AEFs were calculated by comparing against the R6G reference spectrum (Table 1). The vibration modes of R6G molecules corresponding to each Raman shift (discussed above) have also been assigned in each case (Table 1). It was found that, regardless of the type of structure, clear signal enhancement was obtained using the 2PP-printed SERS platforms. Importantly, it should also be noted here that the calculated AEFs are likely to be underestimated since even Al foil exhibits a small SERS effect.

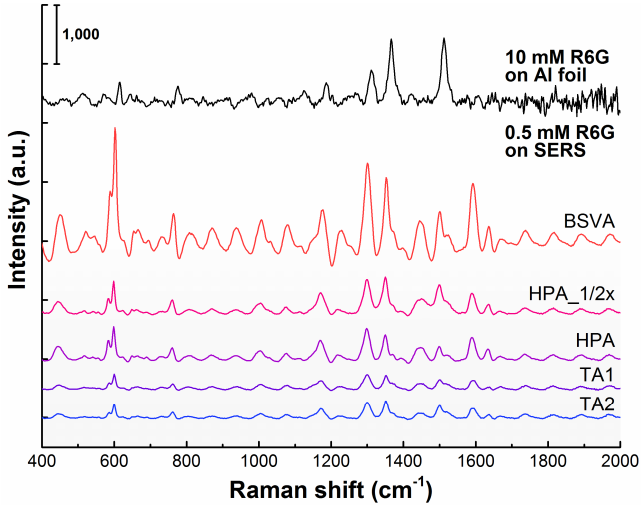

Figure 3. Comparison of the Raman spectra of 0.5 mM R6G aqueous solution on the various SERS micro-structures and the reference spectrum of 10 mM R6G solution on Al foil.

Of all the structures tested, the 2D BSVA with an intervoxel spacing of 0.9 μm exhibited the best enhancement performance (2- to 3-fold higher than the 3D structures). It is also noteworthy that there was no significant difference in AEF between HPA and HPA_1/2x, nor between TA1 and TA2. Together, these observations indicate that, in this case, the 2D distribution of voxels (with a spacing of a = 0.9 μm) was preferable to the more complex 3D structures. As a consequence, these results demonstrate the importance of optimizing the size and spacing of micro-structures (regardless of complexity) in the development of any SERS platform.

Table 1. Characteristic peak wavenumbers of the Raman spectra of R6G, corresponding vibration modes, and calculated normalized AEFs for each SERS micro-structure.

		Normalized AEFs				
Wavenumber (cm^{-1})	**Vibration mode**	BSVA (a = 0.9 μm)	HPA_1/2x	HPA	TA1	TA2
600	C – C – C Ring, in-plane vibration	1,919	535	534	535	229
762	C – H Out-of-plane bending	567	273	216	273	113
1172	C – H In-plane bending	530	346	307	346	156
1300	N – H In-plane bending	810	348	311	348	161
1350	C – C Stretching	333	189	122	189	88
1500		150	146	59	146	63

Downloaded From: https://www.spiedigitallibrary.org/conference-proceedings-of-spie on 11 Mar 2019
Terms of Use: https://www.spiedigitallibrary.org/terms-of-use

3.3 Rapid *E. coli* detection

Following the observation that the BSVA (0.9 µm intervoxel spacing) provided the greatest signal enhancement, the capability of the BSVA for *in vitro* bacteria detection was assessed. Very strong and sharp spectra intermittently appeared over time when bacterial cells swam above the array. An example spectrum collected when *E. coli* were located on the array during the 50 ms acquisition time is shown in Fig. 4. Good signal-to-noise ratio without any post-processing of the spectrum was obtained within the 50 ms acquisition time (5 ms exposure time, average of 10 scans). Additionally, particularly clear peaks were observed at around 1100 cm^{-1} and 1490 cm^{-1}, which are indicative of nucleic acids and lipids[11]. This preliminary data suggests that the SERS platforms presented in this study may have the potential to facilitate rapid recognition of motile bacteria.

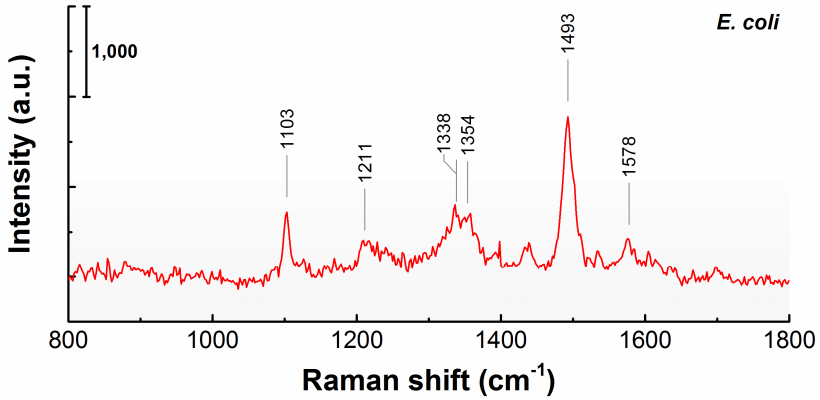

Figure 4. Representative live *E. coli* Raman spectrum recorded using the BSVA SERS microstructure (a = 0.9 µm).

4. CONCLUSION

Various micro-structures fabricated using DLW were proposed to enhance Raman scattering intensity for the purpose of molecular and bacterial sensing. Model geometries from 2D to 3D can be easily realized using 2PP with a high degree of freedom compared to conventional approaches used to produce SERS platforms. A 2D model proposed in this study was designed to generate SERS hot spots at the gaps between single-voxels (BSVA). In addition, 3D models (HPA and TA) were also fabricated and the SERS performance was assessed in each case. Based on R6G measurements, the BSVA exhibited the best performance showing an AEF of up to 2×10^3. The BSVA SERS platform also showed good sensitivity for bacteria detection with a high signal-to-noise ratio observed using a short acquisition time of 50 ms. Consequently, SERS platforms fabricated using DLW show promise for future *in vivo* sensing applications. Generation of smaller features and gaps (to provide improved signal enhancement) is now being investigated by further modifying the configuration and parameters of the DLW process.

REFERENCES

[1] Fries, M., and Steele, A., [Raman Spectroscopy and Confocal Raman Imaging in Mineralogy and Petrography] , in Confocal Raman Microsc., T. Dieing, O. Hollricher, and J. Toporski, Eds., Springer Berlin Heidelberg, Berlin, Heidelberg, 111–135 (2011).

[2] Bokobza, L., Bruneel, J.-L., and Couzi, M., "Raman spectroscopy as a tool for the analysis of carbon-based materials (highly oriented pyrolitic graphite, multilayer graphene and multiwall carbon nanotubes) and of some of their elastomeric composites," Vibrational Spectroscopy 74, 57–63 (2014).

[3] Voronov, O.A., and Street, K.W., "Raman scattering in a new carbon material," Diamond and Related Materials 19(1), 31–39 (2010).

[4] Tiberj, A., and Camassel, J., [Raman Imaging in Semiconductor Physics: Applications to Microelectronic Materials and Devices] , in Raman Imaging Tech. Appl., A. Zoubir, Ed., Springer Berlin Heidelberg, Berlin, Heidelberg, 39–83 (2012).

Downloaded From: https://www.spiedigitallibrary.org/conference-proceedings-of-spie on 11 Mar 2019
Terms of Use: https://www.spiedigitallibrary.org/terms-of-use

[5] Fini, G., "Applications of Raman spectroscopy to pharmacy," Journal of Raman Spectroscopy 35(5), 335–337 (2004).
[6] Sikirzhytski, V., Sikirzhytskaya, A., and Lednev, I.K., "Multidimensional Raman spectroscopic signatures as a tool for forensic identification of body fluid traces: A review," Applied Spectroscopy 65(11), 1223–1232 (2011).
[7] De Oliveira Penido, C.A.F., Pacheco, M.T.T., Lednev, I.K., and Silveira, L., "Raman spectroscopy in forensic analysis: Identification of cocaine and other illegal drugs of abuse," Journal of Raman Spectroscopy 47(1), 28–38 (2016).
[8] Butler, H.J., Ashton, L., Bird, B., Cinque, G., Curtis, K., Dorney, J., Esmonde-White, K., Fullwood, N.J., Gardner, B., et al., "Using Raman spectroscopy to characterize biological materials," Nature Protocols 11(4), 664–687 (2016).
[9] Kong, K., Kendall, C., Stone, N., and Notingher, I., "Raman spectroscopy for medical diagnostics - From in-vitro biofluid assays to in-vivo cancer detection," Advanced Drug Delivery Reviews 89, 121–134 (2015).
[10] Talari, A.C.S., Movasaghi, Z., Rehman, S., and Rehman, I.U., "Raman spectroscopy of biological tissues," Applied Spectroscopy Reviews 50(1), 46–111 (2015).
[11] Shipp, D.W., Sinjab, F., and Notingher, I., "Raman spectroscopy: techniques and applications in the life sciences," Advances in Optics and Photonics 9(2), 315 (2017).
[12] Ding, S.-Y., Yi, J., Li, J.-F., Ren, B., Wu, D.-Y., Panneerselvam, R., and Tian, Z.-Q., "Nanostructure-based plasmon-enhanced Raman spectroscopy for surface analysis of materials," Nature Reviews Materials 1(6), 16021 (2016).
[13] Ouyang, L., Ren, W., Zhu, L., and Irudayaraj, J., "Prosperity to challenges: Recent approaches in SERS substrate fabrication," Reviews in Analytical Chemistry 36(1), (2017).
[14] LeRu, E.C., Meyer, M., Etchegoin, P.G., Le Ru, E.C., and Blackie, E., "Surface Enhanced Raman Scattering Enhancement Factors: A Comprehensive Study," Journal of Physical Chemistry C 111(37), 13794–13803 (2007).
[15] Le Ru, E., and Etchegoin, P., [Principles of Surface Enhanced Raman Spectroscopy and related plasmonic effects] , Elsevier (2009).
[16] Le Ru, E.C., and Etchegoin, P.G., "Quantifying SERS enhancements," MRS Bulletin 38(8), 631–640 (2013).

Downloaded From: https://www.spiedigitallibrary.org/conference-proceedings-of-spie on 11 Mar 2019
Terms of Use: https://www.spiedigitallibrary.org/terms-of-use